JACS
JOURNAL OF THE AMERICAN CHEMICAL SOCIETY
Communication
pubs.acs.org/JACS

X-ray Snapshot Observation of Palladium-Mediated Aromatic Bromination in a Porous Complex

Koki Ikemoto,[†] Yasuhide Inokuma,[†] Kari Rissanen,[‡] and Makoto Fujita*[,†]

[†]Department of Applied Chemistry, School of Engineering, The University of Tokyo, 7-3-1 Hongo, Bunkyo-ku, Tokyo 113-8656, Japan

[‡]Department of Chemistry, NanoScience Center, University of Jyväskylä, P.O. Box 35, 40014 Jyväskylä, Finland

Supporting Information

ABSTRACT: Pd-mediated aromatic bromination is intriguing to synthetic and organometallic chemists due to both its synthetic utility and, more importantly, a proposed mechanism involving an uncommon Pd(IV)/Pd(II) catalytic cycle. Here, we report an X-ray snapshot observation of a Pd reaction center during a Pd-mediated aromatic bromination in a single crystal of a porous coordination network crystalline scaffold. Upon treatment of a single crystal with *N*-bromosuccinimide, sequential X-ray snapshots revealed that the aryl-Pd(II)-L species embedded in the network pores was converted to the brominated aryl product through a transient aryl-Pd(II)-Br species, which is normally unobservable because of its rapid dimerization into insoluble $Pd_2(\mu\text{-}Br)_2$ species. Though the reaction pathway may be biased by the crystalline state, the new X-ray snapshot method relies on crystalline flasks to provide important mechanistic insight.

Transition-metal-mediated reactions continue to play pivotal roles in modern synthetic chemistry and are widely investigated from both synthetic and mechanistic viewpoints.[1] In mechanistic studies, strong evidence or support for a given mechanism is often provided by X-ray crystallographic analysis of a proposed catalytic species, typically prepared separately in a stoichiometric fashion. Crystallization of these intermediates, however, is primarily limited to stable or stabilized representative species. The unisolable transient species actually involved in catalytic cycles have rarely been observed by X-ray diffraction studies outside of time-dependent protein crystallography of metalloenzymes.[2] Here we report a series of X-ray snapshots[3] following the Pd reaction center during a Pd-mediated aromatic bromination[4] occurring within the crystalline scaffold of porous coordination network crystals,[5] which we term "crystalline flasks".[6] An aryl-Pd(II)-L (L = ligand) complex embedded in the pore of the crystalline flask was treated with *N*-bromosuccinimde (NBS). By in situ crystallography, we observed the transient aryl-Pd(II)-Br species, which is normally difficult to isolate and crystallize from a complicated reaction mixture because of its high tendency to dimerize into $Pd_2(\mu\text{-}Br)_2$ species before forming a final brominated aryl product via reductive elimination. The sequential X-ray observation provides important structural evidence, including an elusive intermediate, for the better understanding of Pd-mediated aromatic halogenation, for which both Pd(II)/Pd(0)[7] and Pd(IV)/Pd(II) pathways[8] have been considered.

The crystalline flasks are robust, porous coordination networks that accommodate reactive substrates and reagents within the crystal pores and can thereby institute order and render the reaction intermediates crystallographically observable.[6] For example, we successfully observed the effects of substrate preorganization in a Diels–Alder reaction[9] and a transient hemiaminal intermediate in Schiff base formation,[10] all within the ordered scaffolds of these crystalline flasks. Our method enables the crystallographic analysis of not only stable species but also labile intermediates from reaction mixtures by applying disorder models. We envision that this method could facilitate direct observation of the structural changes undergone by a transition metal catalyst in a mechanistically unclear reaction and thereby shed light on the reaction mechanism. We chose the Pd-mediated aromatic bromination (Figure 1) because of its synthetic utility and, more importantly, because the proposed uncommon Pd(IV)/Pd(II) reaction cycle is of significant interest.[8]

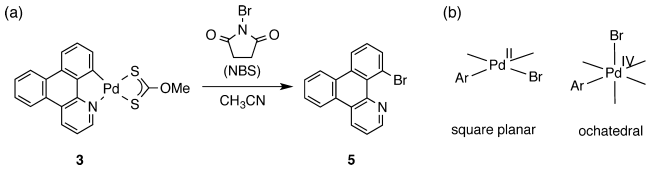

Figure 1. (a) Palladium-mediated aromatic bromination investigated in this work. (b) Plausible reaction intermediates: square-planar Pd(II) and octahedral Pd(IV) species (Ar = aryl).

The framework of the crystalline flask **1** consists of ZnI_2, tris(4-pyridyl)triazine ligand (**2**), and a planar aromatic guest cartridge, typically a triphenylene analogue, which is embedded in the network skeleton via efficient aromatic stacking.[11] In this work, a Pd(II) metal catalyst was attached to a 1-azatriphenylene cartridge. The complexation of $Pd(acac)_2$ (acac = acetylacetonate) by 1-azatriphenylene was followed by ligand exchange with sodium methylxanthate to give the planar aryl-Pd(II) complex **3**, a suitable guest cartridge ready to be inserted into the network scaffold. The strongly coordinating and sterically diminutive methylxanthate ligand was essential

Received: March 25, 2014
Published: May 1, 2014

dx.doi.org/10.1021/ja502996h | J. Am. Chem. Soc. 2014, 136, 6892–6895

for avoiding ligand exchange with ZnI_2 during the network assembly. The desired crystalline flask with intercalated organopalladium complex **1·3** was prepared by slowly layering a methanol solution of ZnI_2 onto a nitrobenzene/methanol solution of ligand **2** and complex **3** (Figure 2a). After 7 days at

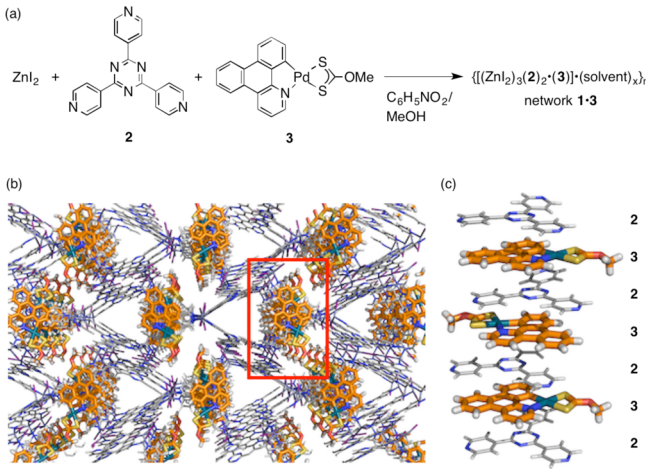

Figure 2. (a) Preparation of organopalladium-embedded porous network complex **1·3**. (b) Crystal structure of as-synthesized **1·3**. (c) Side view of the columnar stack between **2** and **3** at the inserted rectangle in (b).

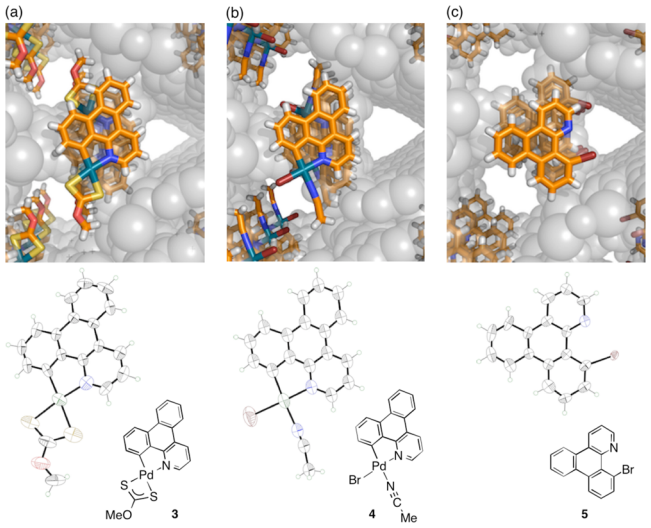

Figure 3. X-ray sequential observation of Pd-mediated C−Br bond formation reaction within the porous coordination network crystal **1·3**. (a) Crystal structure before the reaction. (b) Crystal structure of the observed intermediate within the crystal (conditions: immersed in NBS solution at room temperature for 3 h, washed with acetonitrile, and then allowed to stand at room temperature for 2 h). (c) Crystal structure after the reaction (conditions: immersed in NBS solution at room temperature for 24 h). All thermal ellipsoids are drawn at the 40% probability level.

room temperature, the complex **1·3** was obtained as yellow crystals in 34% yield. The formula was determined to be $\{[(ZnI_2)_3(\mathbf{2})_2\cdot(\mathbf{3})]\cdot(C_6H_5NO_2)_4\}_n$ by elemental analysis. Ultimately, X-ray crystallography revealed that Pd complex **3** was intercalated between two ligands of **2** via $\pi-\pi$ stacking, as expected from previous studies.[11] The Pd center rests within the 1D pores and adopts square-planar coordination geometry, indicative of a Pd(II) oxidation state (Figures 2b,c and 3a).

Successful conditions for bromination of **3** with NBS in the crystalline flask were then determined. The pores of the as-synthesized **1·3** complex are filled with strongly associated nitrobenzene molecules that prevent the smooth diffusion of incoming reagents. Therefore, prior to bromination, residual nitrobenzene in the pores was replaced with acetonitrile by soaking the **1·3** crystals in acetonitrile at room temperature for 3 days. X-ray and ^{1}H NMR analyses confirmed that palladium complex **3** remained intact after the solvent exchange (Figure S1, SI). Crystals **1·3** were then treated with a 0.025 M acetonitrile solution of NBS. After 24 h at room temperature, X-ray crystallographic analysis demonstrated the formation of the final brominated aryl product **5** (Figure 3c).

After confirming that the bromination proceeded cleanly within the pores of the crystalline flask, we used time-dependent X-ray diffraction to capture snapshots of the reaction intermediates. Using the reaction conditions identical to those described above, one crystal was picked up after 3 h and subjected to diffraction study at 90 K. The electron density map revealed that the methylxanthate ligand had dissociated and acetonitrile was now coordinated to the palladium center, preserving the square-planar geometry (Figure S3, SI). Coordination of the acetonitrile ligand was supported by the spectroscopic observation of a new band at 2326 cm^{-1}, attributable to CN stretching in the CH_3CN-Pd structure, by in situ FT-IR spectroscopy (Figure S4, SI).[12] Precise crystallographic identification of the resulting intermediate was hampered at this stage by strong extraneous electron densities in the pores, presumably derived from disordered Br species such as Br_2, BrOH, or Br^- that were unassignable. Thus, we replaced the reaction supernatant with fresh acetonitrile to wash away the unbound species from the pores. After washing, the reaction was monitored by X-ray diffraction at 15 min, 1 h, 2 h, 6 h, and 15 h (Figure S3, SI). At 15 min, the previously unassignable strong electron densities had mostly disappeared.

Time-dependent electron density maps (F_o) obtained from the washed crystals revealed the formation of the Ar−Pd−Br intermediate and its conversion to the Ar−Br product (Figure 4). Although the resolution of the X-ray data was not quite as good as that of conventional single-crystal diffraction data because of there existing several intermediate species and conformations, it was clearly indicated that the electron density at the Pd coordination site trans to the nitrogen donor gradually increased and reached a maximum after 2 h (Figure 4a), suggesting the formation of a Pd−Br bond. The Raman spectrum showed a new band at 163 cm^{-1}, corroborating the presence of a Pd−Br bond in the crystal (Figure S5, SI). The other Pd coordination site was invariably occupied by acetonitrile during the observation period. Multiple C−H···I interactions between the coordinating acetonitrile methyl hydrogens and the ZnI_2 exposed at the surface of the pore were observed (Figure S6, SI). The coordination site trans to that carbon donor was assumed to be more labile, due to the trans effect, but stabilization resulting from the C−H···I interactions might inhibit ligand exchange at the site. Refinement of the diffraction data at 2 h was successful and revealed the formation of intermediate **4** (Figure 3b). Intermediate **4** forms upon treatment with NBS by ligand exchange with bromide, presumably generated by the reduction of NBS with the liberated methylxanthate ion of starting complex **3** (see SI for details).

dx.doi.org/10.1021/ja502996h | J. Am. Chem. Soc. 2014, 136, 6892−6895

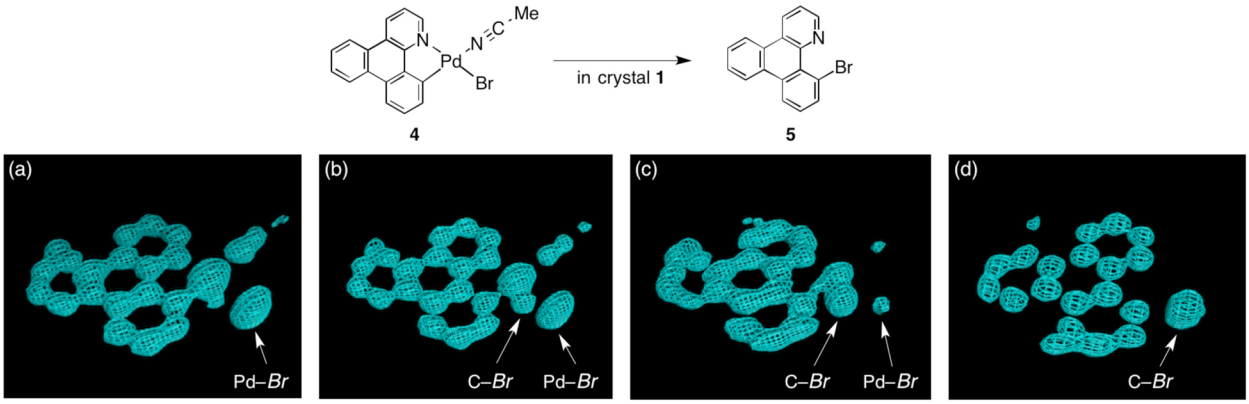

Figure 4. Time-dependent X-ray diffraction data in the conversion from intermediate **4** into final product **5**. (a–c) Electron density maps (F_0) obtained at 2, 6, and 15 h after the wash described in the text and (d) that in the final state (the structure of Figure 3c). The bromine atoms of disappearing Pd–Br and forming C–Br bonds are indicated with arrows. All maps are depicted within 2.5-Å-thick slice of the azatriphenylene moiety and contoured at the absolute 0.95σ level.

We emphasize that single-crystal X-ray observation of monomeric Ar-Pd(X)(CH_3CN) (X = halogen) species, such as intermediate **4**, is rather rare because of the rapid exchange of the weakly donating acetonitrile ligand followed by dimerization into $Pd_2(\mu\text{-}Br)_2$ complexes and precipitation from solution. To the best of our knowledge, only one crystal structure is reported for monocationic Ar-Pd(X)(CH_3CN) (X = halogen) type species in which coulomb repulsion seems to suppress dimerization during the crystallization.[13] However, complex **4** needs only exist for a fleeting moment during the reaction. Accordingly, we were able to directly visualize, via X-ray snapshots, the eventual conversion of intermediate **4** to the final product **5** (Figure 4). Namely, electron density corresponding to the Pd(II)–Br bond gradually disappeared and was replaced with the emergence of density at the aryl–Br bond. Throughout the crystallographic observation of the reaction center, the square-planar geometry of the palladium center was maintained, and no apically coordinated Pd(IV) species were observed. It should be mentioned that our X-ray technique using crystalline flasks has a limitation in that fleeting species with low populations are hardly observed because of their trivial contribution of the changes in the electron density maps. Nevertheless, the most plausible mechanism for the formation of the aryl–Br bond in **5** is reductive elimination from aryl–Pd(II)–Br intermediate **4** (Figure S8, SI). It is also worthy of note that, though the types of ligands are different, Ar–Pd(II)–Br species analogous to intermediate **4** are known to be equilibrated with Ar–Br and Pd(0) species in solution because of reversible reductive elimination–oxidative addition processes.[7b] However, in our reaction system, once compound **4** undergoes reductive elimination, liberated Pd elutes out from the pores of host crystal **1**; thus, aryl bromide **5** is quantitatively obtained in the crystals. In fact, atomic absorption spectrometry showed that 92% of the Pd had eluted into the supernatant after the reaction.

It should be noted that these results are not necessarily conclusive for the Pd-mediated aromatic bromination reaction since the reaction pathway is more or less biased by a crystalline state. First, the formation of dimeric Pd(III)–Pd(III) species,[8f] recently reported to support the Pd(II)/Pd(IV) mechanism, is inhibited in the crystal. Second, the apical positions on the Pd atom in the crystal are blocked by the π-stacking ligand **2** (Figure S7, SI), though the facile slip/slide motion of the triphenylene moiety, observed in our previous studies,[9,10,14] may allow the formation of Pd(IV) species. Third, even though a Pd(IV) species is formed during the reaction, it must have sufficient lifetime; otherwise, it cannot be detected by our X-ray crystallography technique. Therefore, the best interpretation of our results presented here is that the Pd(IV)/Pd(II) mechanism is not exclusive and a Pd(II)/Pd(0) mechanism can also account for Pd-mediated bromination.

Nevertheless, crystallography-based mechanistic studies within crystalline flasks provide important and significant advantages compared to conventional solution-state reactive intermediate structural investigations. First, the isolation of each individual, often unstable species is not necessary because the structure of the reactive intermediate can be determined when severe disorder of the intermediate is not observed. Second, the reaction can be either completely frozen or drastically slowed down at any stage of the reaction by simply cooling the crystal, and thus data collection at various points of the reaction can be done. Therefore, in situ crystallography using crystalline flasks provides a new and highly illuminative tool for the mechanistic studies of transition-metal-mediated reactions that can reveal transient, non-isolable, or non-observable reaction intermediates. Organometallic reactions exhibit a plethora of unknown intermediates, and we believe that in situ crystallography inside crystalline flasks will play an important role in elucidating unknown reaction mechanisms, potentially even those involved in bioinorganic transformations.

■ ASSOCIATED CONTENT

Supporting Information

Detailed experimental procedures, ^{1}H NMR spectra, IR spectra, Raman spectra, and X-ray crystallographic data. This material is available free of charge via the Internet at http://pubs.acs.org.

■ AUTHOR INFORMATION

Corresponding Author

mfujita@appchem.t.u-tokyo.ac.jp

Notes

The authors declare no competing financial interest.

■ ACKNOWLEDGMENTS

This research was supported by Grants-in-Aid for Specially Promoted Research (24000009), of which M.F. is the principal investigator. K.R. thanks the Academy of Finland (grant nos.

265328 and 263256). K.I. thanks the JSPS Research Fellowship for Young Scientists. We thank JASCO Co. for the measurement of Raman spectroscopy.

REFERENCES

(1) (a) Hartwig, J. *Organotransition Metal Chemistry: From Bonding To Catalysis*; University Science Books; Sausalito, CA, 2010. (b) Tsuji, J. *Palladium Reagents and Catalysis: Innovations in Organic Synthesis*; Wiley: Chichester, UK, 1995.
(2) (a) Ren, Z.; Bourgeois, D.; Helliwell, J. R.; Moffat, K.; Šrajer, V.; Stoddard, B. L. J. *Synchrotron Radiat.* **1999**, *6*, 891−917. (b) Moffat, K. *Chem. Rev.* **2001**, *101*, 1569−1581.
(3) (a) Ohashi, Y. *Acta Crystallogr.* **1998**, *A54*, 842−849. (b) Coppens, P.; Vorontsov, I. I.; Graber, T.; Gembicky, M.; Kovalevsky, A. Y. *Acta Crystallogr.* **2005**, *A61*, 162−172.
(4) (a) Vigalok, A. *Chem.—Eur. J.* **2008**, *14*, 5102−5108. (b) Sheppard, T. D. *Org. Biomol. Chem.* **2009**, *7*, 1043−1052. (c) Lyons, T. W.; Sanford, M. S. *Chem. Rev.* **2010**, *110*, 1147−1169.
(5) (a) Moulton, B.; Zaworotko, M. J. *Chem. Rev.* **2001**, *101*, 1629−1658. (b) Yaghi, O. M.; O'Keeffe, M.; Ockwig, N. W.; Chae, H. K.; Eddaoudi, M.; Kim, J. *Nature* **2003**, *423*, 705−714. (c) Kitagawa, S.; Kitaura, R.; Noro, S. *Angew. Chem., Int. Ed.* **2004**, *43*, 2334−2375. (d) Férey, G. *Chem. Soc. Rev.* **2008**, *37*, 191−214. (e) Wang, Z.; Cohen, S. M. *Chem. Soc. Rev.* **2009**, *38*, 1315−1329. (f) Lee, J.; Farha, O. K.; Roberts, J.; Scheidt, K. A.; Nguyen, S. T.; Hupp, J. T. *Chem. Soc. Rev.* **2009**, *38*, 1450−1459.
(6) Inokuma, Y.; Kawano, M.; Fujita, M. *Nat. Chem.* **2011**, *3*, 349−358.
(7) (a) Roy, A. H.; Hartwig, J. F. *J. Am. Chem. Soc.* **2001**, *123*, 1232−1233. (b) Roy, A. H.; Hartwig, J. F. *J. Am. Chem. Soc.* **2003**, *125*, 13944−13945. (c) Watson, D. A.; Su, M.; Teverovskiy, G.; Zhang, Y.; García-Fortanet, J.; Kinzel, T.; Buchwald, S. L. *Science* **2009**, *325*, 1661−1664. (d) Shen, X.; Hyde, A. M.; Buchwald, S. L. *J. Am. Chem. Soc.* **2010**, *132*, 14076−14078. (e) Liu, H.; Li, C.; Qiu, D.; Tong, X. *J. Am. Chem. Soc.* **2011**, *133*, 6187−6193. (f) Newman, S. G.; Howell, J. K.; Nicolaus, N.; Lautens, M. *J. Am. Chem. Soc.* **2011**, *133*, 14916−14919. (g) Petrone, D. A.; Lischka, M.; Lautens, M. *Angew. Chem., Int. Ed.* **2013**, *52*, 10635−10638.
(8) (a) Muñiz, K. *Angew. Chem., Int. Ed.* **2009**, *48*, 9412−9423. (b) Sehnal, P.; Taylor, R. J. K.; Fairlamb, I. J. S. *Chem. Rev.* **2010**, *110*, 824−889. (c) Xu, L.-M.; Li, B.-J.; Yang, Z.; Shi, Z.-J. *Chem. Soc. Rev.* **2010**, *39*, 712−733. (d) Dick, A. R.; Hull, K. L.; Sanford, M. S. *J. Am. Chem. Soc.* **2004**, *126*, 2300−2301. (e) Whitfield, S. R.; Sanford, M. S. *J. Am. Chem. Soc.* **2007**, *129*, 15142−15143. (f) Powers, D.; Ritter, T. *Nat. Chem.* **2009**, *1*, 302−309.
(9) Ikemoto, K.; Inokuma, Y.; Fujita, M. *J. Am. Chem. Soc.* **2011**, *133*, 16806−16808.
(10) Kawamichi, T.; Haneda, T.; Kawano, M.; Fujita, M. *Nature* **2009**, *461*, 633−635.
(11) Fornies, J.; Navarro, R.; Sicilia, V. *Polyhedron* **1988**, *7*, 2659−2665.
(12) Kawano, M.; Kawamichi, T.; Haneda, T.; Kojima, T.; Fujita, M. *J. Am. Chem. Soc.* **2007**, *129*, 15418−15419.
(13) Strong, E. T. J.; Price, J. T.; Jones, N. D. *Dalton Trans.* **2009**, *2*, 9123−9125.
(14) Kawamichi, T.; Kodama, T.; Kawano, M.; Fujita, M. *Angew. Chem., Int. Ed.* **2008**, *47*, 8030−8032.